ACS MATERIALS LETTERS

www.acsmaterialsletters.org

Precise Hydrogen Sieving by Carbon Molecular Sieve Membranes Derived from Solution-Processable Aromatic Polyamides

Gaurav M. Iyer and Chen Zhang*

Cite This: *ACS Materials Lett.* 2023, 5, 243−248

Read Online

ACCESS | Metrics & More | Article Recommendations | Supporting Information

ABSTRACT: Aromatic polyamides (aramids) are broadly used to manufacture desalination membranes; however, they are rarely considered for gas separation. Here, we report precise hydrogen sieving in ultramicroporous carbon molecular sieve (CMS) membranes derived from an uncrosslinked aramid synthesized by stirred interfacial polymerization of diamine and mixed diacid chloride monomers. While hydrogen bonds gave the aramid precursor unattractive separation performance, they were leveraged to provide aramid-derived CMS membranes with ultrahigh H_2/CO_2 selectivity exceeding all known CMS membranes. Adsorption in aramid-derived CMS membranes suggested their ultrahigh H_2/CO_2 selectivity was attributable to diffusion selectivity above 3000. The excellent solution processability of uncrosslinked aramids allowed the fabrication of scalable CMS hollow fiber membranes. The findings of this work open the door to a new class of highly selective CMS membranes for H_2 separation and CO_2 capture.

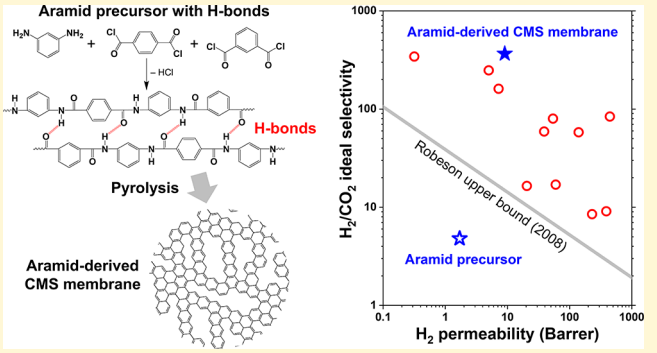

The chemistry of polymer precursors is known to govern the pore structure and transport properties of carbon molecular sieve (CMS) membranes.[1] As a polymer precursor is pyrolyzed, rigid aromatic strands are formed and organize into defective plates to provide disordered three-dimensional micropores.[2] Many polymer precursors have been studied to fabricate CMS membranes, including polyimides,[3] polymers of intrinsic microporosity (PIMs),[4,5] and polybenzimidazoles (PBIs).[6,7] By controlling the backbone and bulky side group chemistry of the polymer precursor, the plate defects (i.e., ultramicropores) can be tuned to control molecular discrimination and to obtain attractive gas,[8−11] vapor,[12] and liquid[13] separation performance exceeding polymer membranes and many other molecular sieve membranes. Notably, CMS membranes can recover hydrogen (H_2) and capture carbon dioxide (CO_2) to enable sustainable production of blue H_2 from steam methane reforming.[4] Precise H_2 sieving and outstanding H_2/CO_2 selectivity is required in H_2-selective CMS membranes to produce a high-purity H_2 product stream.

To the best of our knowledge, no CMS membranes have been reported based on aromatic polyamides (aramids).[14] This is surprising because aramids represent the most broadly practiced and well-known polymer membrane materials.[15−17] Aramids can be inexpensively and rapidly synthesized at room temperature by in situ interfacial polymerization on a substrate or stirred interfacial polymerization in a solution. Aramid chemistry is highly tunable through a rich library of multifunctional amine and acid chloride monomers.[18] Notably, defect-free ultrathin aramid films made by in situ interfacial polymerization of *m*-phenylenediamine (MPD) and trimesoyl chloride (TMC) can provide thin-film composite reverse osmosis membranes with attractive water flux and salt rejection.[15,19] However, aramids are conventionally seen as unsuitable for gas separations. They are known to have low gas permeabilities[20−22] at ambient temperature under dry gas feeds[23] and usually considered as barrier materials,[24] because of their strong hydrogen bonds and low fractional free volume (FFV). Hydrogen/hydrocarbon separation is the only known commercial gas separation application of aramid membranes.[25]

In this work, we show that pyrolysis of solution-processable aramids can provide CMS membranes with precise H_2 sieving and outstanding H_2/CO_2 selectivity. Crosslinked aramids are

Received: October 29, 2022
Accepted: December 13, 2022
Published: December 20, 2022

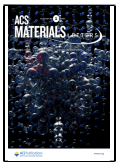

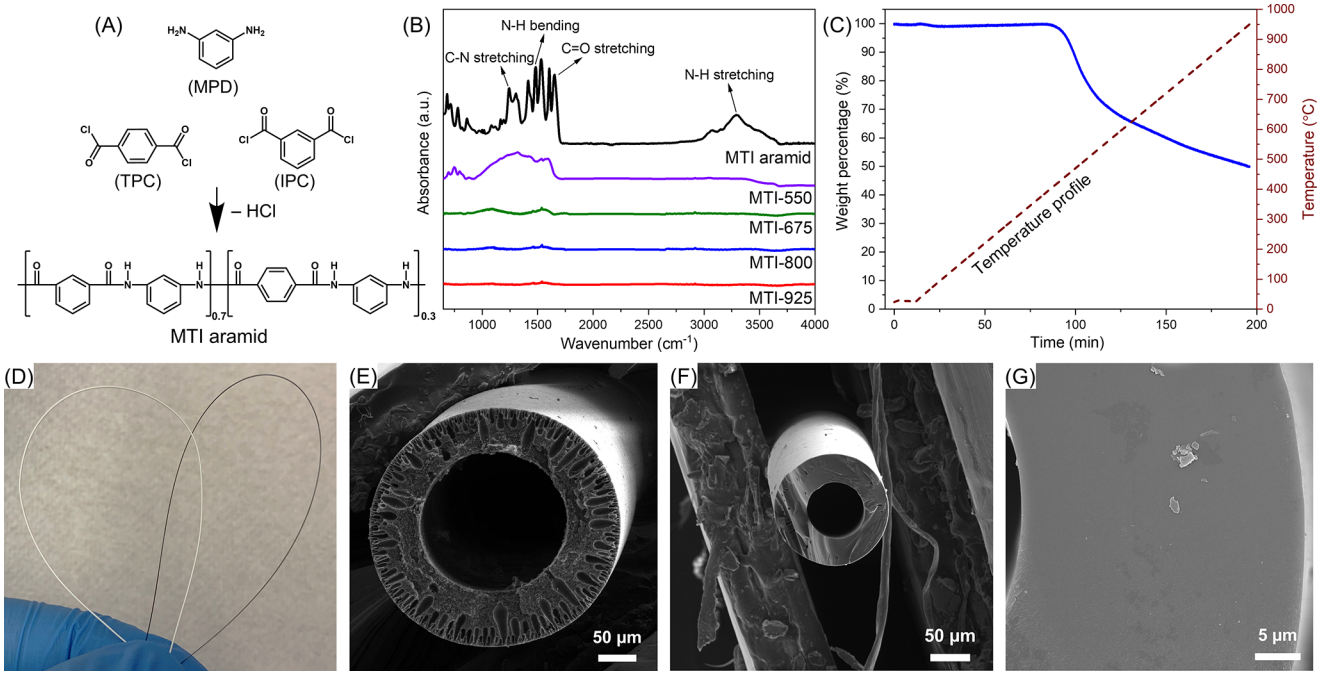

Figure 1. (A) Synthetic route of the MTI aramid. (B) FT-IR spectra of the MTI aramid and aramid-derived CMS membranes. (C) TGA curve of the MTI aramid under nitrogen purge. (D) Photograph showing the excellent flexibility of the aramid hollow fiber (white) and aramid-derived CMS hollow fiber (black). SEM images of (E) aramid hollow fiber, (F) aramid-derived CMS hollow fiber, and (G) dense wall of aramid-derived CMS hollow fiber.

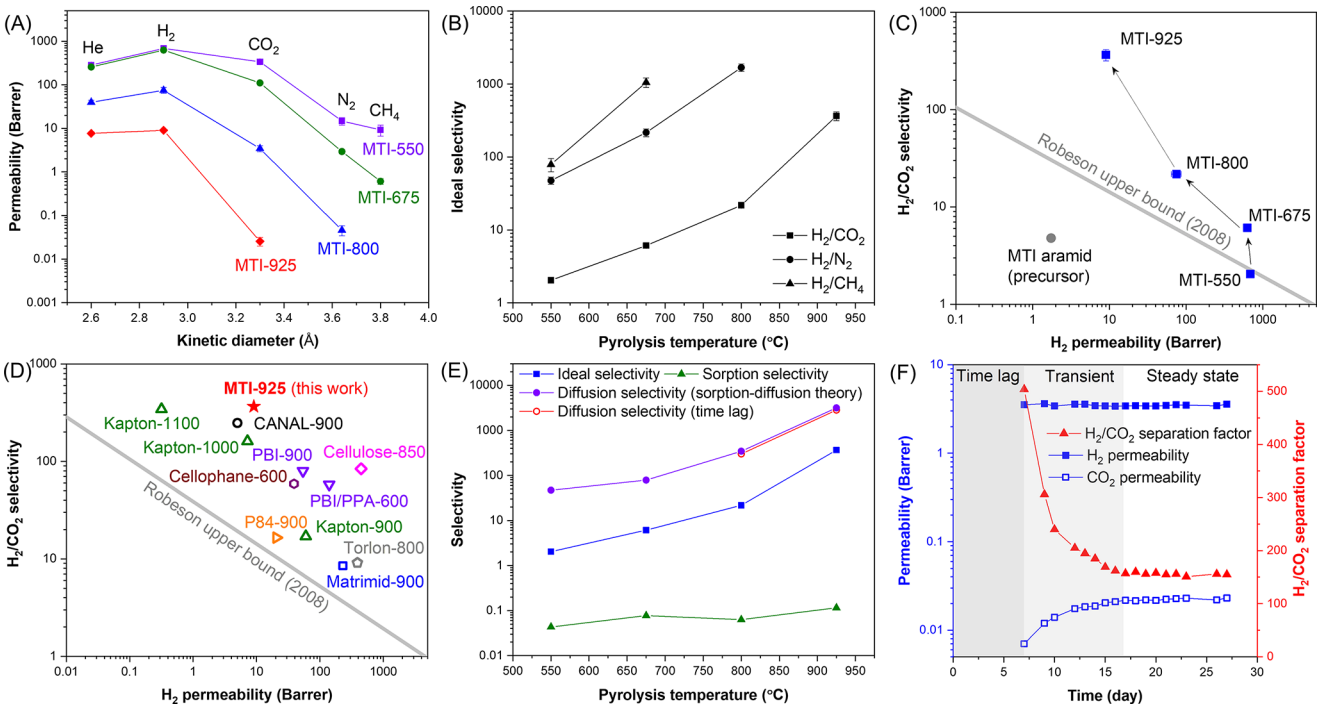

Figure 2. (A) Pure gas permeability and (B) ideal selectivity in aramid-derived CMS membranes. (C) Pure gas H_2/CO_2 separation performance of the MTI aramid precursor and aramid-derived CMS membranes. (D) Comparing the H_2/CO_2 separation performance of aramid-derived CMS membrane (MTI-925) with CMS membranes reported in the literature. (E) The effect of pyrolysis temperature on H_2/CO_2 ideal selectivity, diffusion selectivity, and sorption selectivity in aramid-derived CMS membranes. (F) Mixed-gas H_2/CO_2 permeation in MTI-925 using an equimolar H_2/CO_2 mixture.

often favored over uncrosslinked aramids for desalination, because of their superior monovalent ion rejection.[26] However, crosslinked aramids cannot be solution-processed into films or hollow fibers for CMS membrane formation.[27] In addition, aramid films formed by in situ interfacial polymerization are known to be asymmetric,[28] which prevents unambiguous determination of the thickness and intrinsic transport properties of the CMS membranes derived thereof. To circumvent

https://doi.org/10.1021/acsmaterialslett.2c01029
ACS Materials Lett. 2023, 5, 243−248

these challenges of crosslinked aramids, we synthesized an uncrosslinked aramid (MTI) by stirred interfacial polymerization,[29,30] using MPD as the aqueous phase monomer and a mixture of terephthaloyl chloride (TPC) and isophthaloyl chloride (IPC) as organic phase monomers (Figure 1A). Mixing TPC and IPC (in a ratio of 3:7) reduced the polymer backbone symmetry,[31] giving an amorphous polymer that can be dissolved in strong polar aprotic solvents (see Table S1 in the Supporting Information).

The aramid formation was evidenced by Fourier transform infrared (FT-IR) spectroscopy (Figure 1B) with peaks appearing at 1248 cm^{-1} (C−N stretching), 1477 cm^{-1} (N−H bending), 1659 cm^{-1} (C═O stretching, hydrogen-bonded), and 3311 cm^{-1} (N−H stretching, hydrogen-bonded).

The synthesized MTI aramid was dissolved in dimethylacetamide and made into dense films (see Figure S1 in the Supporting Information) by solution casting. The hydrogen bonds and lack of bulky side groups gave the aramid low FFV (0.057), in addition to unattractive H_2/CO_2 separation performance below the 2008 Robeson upper bound[32] with H_2 permeability of 1.7 Barrer and H_2/CO_2 ideal selectivity of 4.8 at 35 °C. Differential scanning calorimetry (Figure S2 in the Supporting Information) suggested that the aramid had a glass transition temperature of ∼275 °C. Thermogravimetric analysis (TGA) showed that the aramid decomposed at 460 °C in nitrogen with a high carbon residual (∼72% at 550 °C) (see Figure 1C).

The MTI aramid dense films were used as precursors to fabricate CMS dense films, which showed significant curling (see Figure S1), preventing gas permeation measurements. The solution processability of the MTI aramid allowed the fabrication of hollow fibers (outer diameter of ∼330 μm; see Figures 1D and 1E) by dry-jet/wet-quench spinning (see Table S2 in the Supporting Information).[31] The aramid hollow fibers were used as precursors to provide four aramid-derived CMS hollow fiber membranes (MTI-550, MTI-675, MTI-800, and MTI-925) via pyrolysis at 550, 675, 800, and 925 °C, respectively. Several low-intensity peaks were seen in the FT-IR spectra (800−1600 cm^{-1}) of MTI-550 (Figure 1B), suggesting the polymer decomposition was incomplete at 550 °C. The peaks became weaker in MTI-675 and MTI-800 and disappeared in MTI-925, which indicated complete aramid decomposition. Both the aramid hollow fibers and aramid-derived CMS hollow fibers had excellent flexibility (Figure 1D). The pores in the aramid precursor hollow fibers collapsed during pyrolysis, thereby giving dense-wall CMS hollow fiber membranes (Figures 1E and 1F) with an outer diameter of ∼140 μm. The thickness (∼40 μm) of the dense wall (separation layer) can be unambiguously determined to allow gas permeability measurements.[3]

Pure gas permeation of helium (He, d_k [kinetic diameter] = 2.6 Å), hydrogen (H_2, d_k = 2.89 Å), carbon dioxide (CO_2, d_k = 3.3 Å), nitrogen (N_2, d_k = 3.64 Å), and methane (CH_4, d_k = 3.8 Å) was performed in the dense-wall aramid-derived CMS hollow fiber membranes at 35 °C and 10 bar. Permeability reduced as the pyrolysis temperature increased (see Figure 2A, as well as Table S3 in the Supporting Information). The decrease in permeabilities of CO_2, N_2, and CH_4 was more sensitive than H_2 to pyrolysis temperature. Therefore, the H_2/CO_2, H_2/N_2, and H_2/CH_4 ideal selectivities were significantly enhanced at higher pyrolysis temperature (Figure 2B). All aramid-derived CMS membranes showed He permeability that was lower than H_2 permeability. While He has a slightly smaller kinetic diameter, it is less condensable than H_2. In fact, many nonperfluorinated polymer membranes[32] and CMS membranes[3] show He/H_2 selectivity of <1.

The aramid-derived CMS membranes showed particularly competitive H_2/CO_2 separation performance (Figure 2C). Following pyrolysis at 550 °C, the aramid-derived CMS membrane (MTI-550) showed more than 400 times higher H_2 permeability than the MTI aramid precursor, which can be attributed to the formation of CMS micropores. As the pyrolysis temperature further increased, the H_2 permeability decreased with enhanced H_2/CO_2 ideal selectivity. Notably, the CMS membrane pyrolyzed at 925 °C (MTI-925) had H_2/CO_2 separation performance well above the 2008 Robeson upper bound[32] with H_2 permeability of 9.1 Barrer and H_2/CO_2 ideal selectivity of 366, which were ∼5 times and ∼76 times higher than the MTI aramid precursor, respectively.

To our best knowledge, MTI-925 had the highest H_2/CO_2 ideal selectivity among all known CMS membranes (see Figure 2D, as well as Table S4 in the Supporting Information), which include those derived from polyimides (Kapton, Matrimid),[33] polyimide-amides (Torlon),[34] PBIs,[6,7] PIMs,[4] and cellulose.[35,36] Additionally, MTI-925 had competitive H_2 permeability among CMS membranes with H_2/CO_2 ideal selectivity above 100. Kapton-derived CMS membranes[33] showed comparable H_2/CO_2 ideal selectivity; however, they were pyrolyzed at higher temperature (1100 °C) and had much lower H_2 permeability (∼0.32 Barrer).

Sorption of H_2 and CO_2 was studied in the aramid-derived CMS membranes (see Figure S3 in the Supporting Information) at 35 °C to deconvolute the contribution of sorption selectivity and diffusion selectivity. The CO_2 and H_2 sorption isotherms were fit with the dual-mode sorption model[37] and Henry's law, respectively. Indeed, H_2 sorption in porous carbon appeared linear at room temperature at pressures up to 30 bar.[38] The obtained sorption constants (Table S5 in the Supporting Information) allow the determination of H_2/CO_2 diffusion selectivities (Figure 2E), according to the sorption-diffusion theory using measured H_2/CO_2 ideal selectivities. For MTI-800 and MTI-925, H_2/CO_2 diffusion selectivities were also determined independently using the time-lag method (see Figure S4 in the Supporting Information),[39] which had excellent agreement with those determined by the sorption-diffusion theory.

As the pyrolysis temperature increased, the H_2/CO_2 diffusion selectivity dramatically increased from 46 (MTI-550) to 3052 (MTI-925), which was possibly because the CMS ultramicropores became smaller (i.e., ultramicropore tightening).[40] The highly condensable CO_2 sorbs more strongly than H_2 giving H_2/CO_2 sorption selectivities well below 1. Interestingly, MTI-925 had much lower CO_2 sorption capacity than those pyrolyzed at lower temperatures. The reduced CO_2 sorption capacity caused the H_2/CO_2 sorption selectivity to rise by 170% from 0.043 (MTI-550) to 0.116 (MTI-925), which contributed to the ultrahigh H_2/CO_2 ideal selectivity in MTI-925. The reduction in CO_2 sorption capacity and, hence, synergistically increased H_2/CO_2 sorption selectivity can presumably be attributed to the formation of "H_2-selective micropores", only allowing the smaller H_2 molecules to sorb but excluding the larger CO_2 molecules.[3] These H_2-selective micropores were formed possibly by ultramicropore tightening as the CMS structure became more ordered and graphitic at higher pyrolysis temperature.

https://doi.org/10.1021/acsmaterialslett.2c01029
ACS Materials Lett. 2023, 5, 243−248

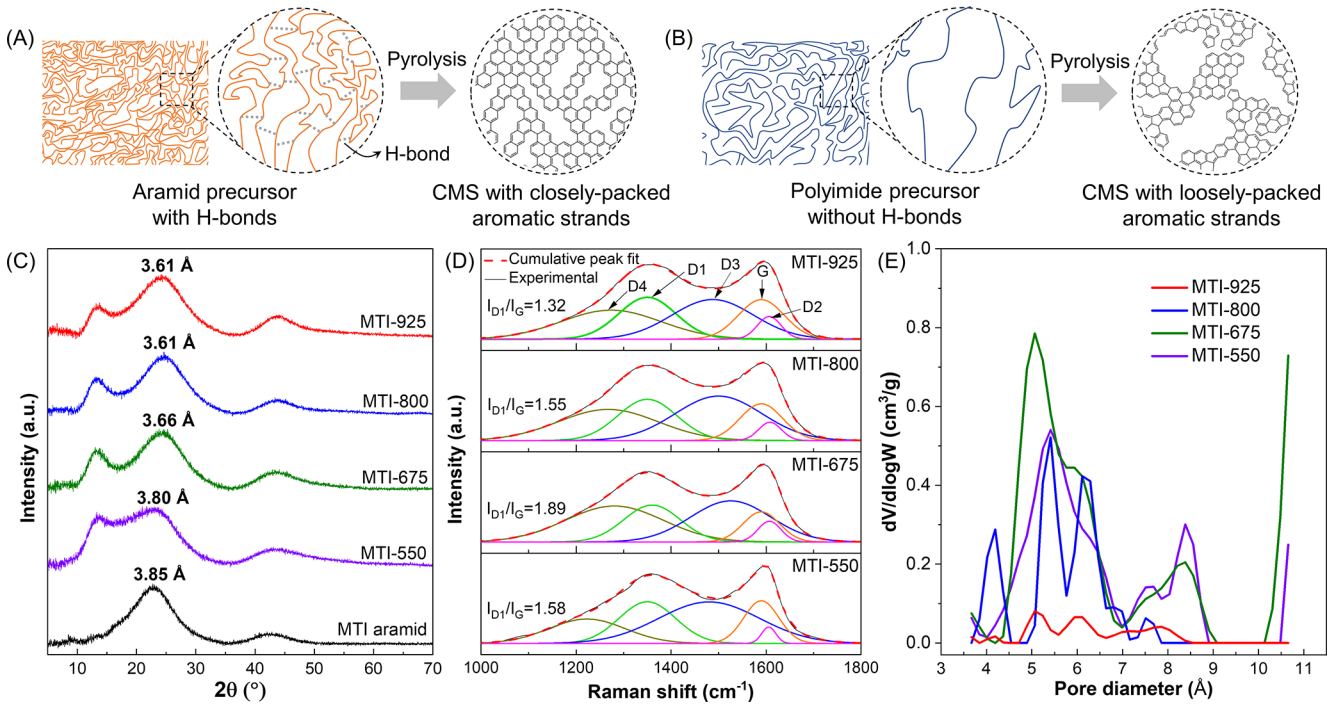

Figure 3. Schematics illustrating the development of CMS membrane ultramicropores using (A) aramid precursor and (B) polyimide precursor. (C) WAXD patterns of the MTI aramid and aramid-derived CMS membranes. (D) Raman spectra of aramid-derived CMS membranes. (E) Pore size distribution of aramid-derived CMS membranes.

We performed mixed gas permeation (Figure 2F) in MTI-925 using an equimolar H_2/CO_2 mixture (2 bar) at 35 °C. Once steady-state permeation was reached, the aramid-derived CMS membrane showed stable H_2 permeability of 3.5 Barrer and a H_2/CO_2 separation factor of 156. The separation factor was lower than the H_2/CO_2 ideal selectivity measured under pure gas permeation. This fact notwithstanding, MTI-925 still gave one of the highest H_2/CO_2 separation factors among all known CMS membranes (see Figure S5 and Table S6 in the Supporting Information). The lower H_2/CO_2 separation factor was possibly due to the competitive CO_2 sorption effect under mixture permeation. We expect the H_2 permeability and H_2/CO_2 separation factor will both rise at higher permeation temperature due to mitigated competitive sorption.[35] Note that the mixture permeation showed longer transient time than pure gas CO_2 permeation (Figure S4D in the Supporting Information). Similar phenomena were observed by Hazazi and co-workers[4] in a ladder polymer-derived CMS membrane.

Interestingly, the aramid-derived CMS membrane (MTI-925) showed more than ten times higher H_2/CO_2 selectivity (Figure 2D) than CMS membranes derived from polyimides (e.g., Matrimid) at similar pyrolysis temperature (900 °C). The MTI aramid precursor has strong hydrogen bonds and, hence, closer chain packing (Figure 3A) than polyimides (Figure 3B). This was evidenced by wide-angle X-ray diffraction (WAXD, Figure 3C) showing that the MTI aramid had smaller average *d*-spacing (~3.85 Å) than Matrimid (~5.58 Å).[3] The closer chain packing in the aramid presumably provided more intimately spaced aromatic strands following pyrolysis, thereby giving smaller ultramicropores and higher H_2/CO_2 selectivity in aramid-derived CMS membranes (Figure 3A). Indeed, the MTI-925 showed smaller average *d*-spacing (~3.61 Å, Figure 3C) than the CMS membrane (~3.86 Å) derived from Matrimid at 900 °C.[3]

The average *d*-spacing calculated from the main diffraction peak position reduced as the pyrolysis temperature of aramid-derived CMS membrane increased from 550 °C to 800 °C, suggesting tightening of the CMS membrane pore structure. Although MTI-925 showed identical average *d*-spacing with MTI-800, MTI-925 had a stronger secondary diffraction peak at $2\theta \approx 44°$, corresponding to the (100) lattice plane of graphite,[2] which indicates a more ordered graphitic structure. Therefore, the results of WAXD corroborate with permeation results that the CMS ultramicropore structure was tightened at higher pyrolysis temperature. Formation of a more ordered and compact carbon structure was further evidenced by higher density of CMS membranes made at higher pyrolysis temperature (Figure S6 in the Supporting Information).

Raman spectra (Figure 3D) of aramid-derived CMS membranes showed a D-band (~1355 cm^{-1}) and a G-band (~1575 cm^{-1}) characteristic of carbon materials. The spectra were deconvoluted into five bands, i.e., D1, D2, D3, D4, and G by Gaussian function.[2,41] The D1 and G band intensity ratio (I_{D1}/I_G) represents the relative concentration of sp^3- and sp^2-hybridized carbons. MTI-675 showed higher I_{D1}/I_G ratio than MTI-550, suggesting MTI-675 is richer in sp^3-hybridized carbon. This is consistent with FT-IR results that the polymer precursor decomposition was incomplete at 550 °C. As the pyrolysis temperature increased to 925 °C, the I_{D1}/I_G ratio reduced, suggesting higher concentrations of sp^2-hybridized carbon and, hence, a more-ordered graphitic structure agreeing with the WAXD and density measurement results.

The pore size distribution (Figure 3E), pore surface area, and pore volume (Figure S7 in the Supporting Information) in aramid-derived CMS membranes were obtained using the density functional theory (DFT) based on CO_2 physisorption isotherms measured at 0 °C. A strong peak appeared in MTI-800 at ~4 Å, suggesting tightening of ultramicropores.

https://doi.org/10.1021/acsmaterialslett.2c01029
ACS Materials Lett. 2023, 5, 243−248

Interestingly, the measured pore volume was significantly reduced in MTI-925 with almost no ultramicropores smaller than 4.5 Å. While this appeared to be inconsistent with permeation results, it can be explained by the aforementioned H_2-selective micropores. As they cannot be accessed by CO_2 molecules due to exclusion, these H_2-selective micropores are not measurable by CO_2 physisorption. While CO_2 physisorption is broadly used to study carbon pore structure,[42] the findings of this work indicate that this approach may not be suitable for CMS membranes with ultrahigh H_2/CO_2 selectivities.

In summary, we show that pyrolysis of a low-permeability aramid can provide CMS membranes with highly attractive gas separation performance. An uncrosslinked aramid was synthesized by stirred interfacial polymerization. The aramid's excellent solution processability allowed the fabrication of aramid precursor hollow fibers by solution spinning, which gave dense-wall CMS hollow fiber membranes. Pure gas permeation suggested that the aramid-derived CMS membrane pyrolyzed at 925 °C (MTI-925) had competitive H_2 permeability and ultrahigh H_2/CO_2 ideal selectivity of 366. The aramid-derived CMS membrane also showed an outstanding H_2/CO_2 separation factor (~156) under H_2/CO_2 mixture permeation tests, suggesting their promise for H_2 purification and CO_2 capture applications. We postulate that the highly attractive H_2/CO_2 separation performance originates from the aramid precursor hydrogen bonds that gave small ultramicropores in aramid-derived CMS membranes. To the best of our knowledge, this is the first report of CMS membranes derived from aramids or interfacially polymerized polymers. The findings of this work pave the way for a new class of scalable and tunable CMS membranes for separations.

■ ASSOCIATED CONTENT

Supporting Information

The Supporting Information is available free of charge at https://pubs.acs.org/doi/10.1021/acsmaterialslett.2c01029.

Experimental procedures regarding synthesis of MTI aramid; fabrication of aramid hollow fibers and aramid dense films; formation of aramid-derived CMS hollow fiber membranes; permeation measurements; equilibrium sorption measurements; and characterizations (scanning electron microscopy, Fourier transform infrared spectroscopy, differential scanning calorimetry, thermogravimetric analysis, density measurement, wide-angle X-ray diffraction, Raman spectroscopy); supplementary text; supplementary figures and tables (PDF)

■ AUTHOR INFORMATION

Corresponding Author

Chen Zhang − *Department of Chemical and Biomolecular Engineering, University of Maryland, College Park, Maryland 20742, United States;* orcid.org/0000-0002-0071-2898; Email: czhang71@umd.edu

Author

Gaurav M. Iyer − *Department of Chemical and Biomolecular Engineering, University of Maryland, College Park, Maryland 20742, United States*

Complete contact information is available at: https://pubs.acs.org/10.1021/acsmaterialslett.2c01029

Author Contributions

The manuscript was written through contributions of all authors. All authors have given approval to the final version of the manuscript. CRediT: **Gaurav M. Iyer** data curation, formal analysis, investigation, methodology, validation, writing-original draft, writing-review & editing; **Chen Zhang** conceptualization, funding acquisition, project administration, resources, supervision, visualization, writing-original draft, writing-review & editing.

Funding

This work is supported by funding from the National Science Foundation (CBET Award No. 1928325).

Notes

The authors declare the following competing financial interest(s): The authors are inventors of a U.S. patent application submitted by the University of Maryland.

■ ACKNOWLEDGMENTS

G.M.I. acknowledges the Harry K. Wells Fellowship provided through the Maryland Energy Innovation Institute. C.Z. thanks additional faculty summer support from the Minta Martin Foundation. The authors thank D. Liu for kindly providing access to the TGA instrument.

■ REFERENCES

(1) Kiyono, M.; Williams, P. J.; Koros, W. J. Effect of polymer precursors on carbon molecular sieve structure and separation performance properties. *Carbon* **2010**, *48* (15), 4432−4441.

(2) Qiu, W.; Leisen, J. E.; Liu, Z.; Quan, W.; Koros, W. J. Key Features of Polyimide-Derived Carbon Molecular Sieves. *Angew. Chem., Int. Ed.* **2021**, *60* (41), 22322−22331.

(3) Zhang, C.; Koros, W. J. Ultraselective Carbon Molecular Sieve Membranes with Tailored Synergistic Sorption Selective Properties. *Adv. Mater.* **2017**, *29* (33), 1701631.

(4) Hazazi, K.; Wang, Y.; Bettahalli, N. M. S.; Ma, X.; Xia, Y.; Pinnau, I. Catalytic arene-norbornene annulation (CANAL) ladder polymer derived carbon membranes with unparalleled hydrogen/carbon dioxide size-sieving capability. *J. Membr. Sci.* **2022**, *654*, 120548.

(5) Ma, Y.; Jue, M. L.; Zhang, F.; Mathias, R.; Jang, H. Y.; Lively, R. P. Creation of Well-Defined "Mid-Sized" Micropores in Carbon Molecular Sieve Membranes. *Angew. Chem., Int. Ed.* **2019**, *58* (38), 13259−13265.

(6) Hu, L.; Bui, V. T.; Krishnamurthy, A.; Fan, S.; Guo, W.; Pal, S.; Chen, X.; Zhang, G.; Ding, Y.; Singh, R. P.; Lupion, M.; Lin, H. Tailoring sub-3.3 Å ultramicropores in advanced carbon molecular sieve membranes for blue hydrogen production. *Sci. Adv.* **2022**, *8* (10), No. eabl8160.

(7) Omidvar, M.; Nguyen, H.; Huang, L.; Doherty, C. M.; Hill, A. J.; Stafford, C. M.; Feng, X.; Swihart, M. T.; Lin, H. Unexpectedly Strong Size-Sieving Ability in Carbonized Polybenzimidazole for Membrane H_2/CO_2 Separation. *ACS Appl. Mater. Interfaces* **2019**, *11* (50), 47365−47372.

(8) Zhang, C.; Kumar, R.; Koros, W. J. Ultra-thin skin carbon hollow fiber membranes for sustainable molecular separations. *AIChE J.* **2019**, *65* (8), No. e16611.

(9) Liu, L.; Liu, D.; Zhang, C. High-temperature hydrogen/propane separations in asymmetric carbon molecular sieve hollow fiber membranes. *J. Membr. Sci.* **2022**, *642*, 119978.

(10) Zhang, C.; Wenz, G. B.; Williams, P. J.; Mayne, J. M.; Liu, G.; Koros, W. J. Purification of Aggressive Supercritical Natural Gas Using Carbon Molecular Sieve Hollow Fiber Membranes. *Ind. Eng. Chem. Res.* **2017**, *56* (37), 10482−10490.

(11) Cao, Y.; Zhang, K.; Sanyal, O.; Koros, W. J. Carbon Molecular Sieve Membrane Preparation by Economical Coating and Pyrolysis of

Porous Polymer Hollow Fibers. *Angew. Chem., Int. Ed.* **2019**, *58* (35), 12149−12153.
(12) Ma, X.; Lin, Y. S.; Wei, X.; Kniep, J. Ultrathin carbon molecular sieve membrane for propylene/propane separation. *AIChE J.* **2016**, *62* (2), 491−499.
(13) Koh, D.-Y.; McCool, B. A.; Deckman, H. W.; Lively, R. P. Reverse osmosis molecular differentiation of organic liquids using carbon molecular sieve membranes. *Science* **2016**, *353* (6301), 804−807.
(14) Jones, C. W.; Koros, W. J. Carbon molecular sieve gas separation membranes-I. Preparation and characterization based on polyimide precursors. *Carbon* **1994**, *32* (8), 1419−1425.
(15) Petersen, R. J. Composite reverse osmosis and nanofiltration membranes. *J. Membr. Sci.* **1993**, *83* (1), 81−150.
(16) Greenlee, L. F.; Lawler, D. F.; Freeman, B. D.; Marrot, B.; Moulin, P. Reverse osmosis desalination: Water sources, technology, and today's challenges. *Water Res.* **2009**, *43* (9), 2317−2348.
(17) Koros, W. J.; Zhang, C. Materials for next-generation molecularly selective synthetic membranes. *Nat. Mater.* **2017**, *16* (3), 289−297.
(18) García, J. M.; García, F. C.; Serna, F.; de la Peña, J. L. High-performance aromatic polyamides. *Prog. Polym. Sci.* **2010**, *35* (5), 623−686.
(19) Ren, J.; Chowdhury, M. R.; Qi, J.; Xia, L.; Huey, B. D.; McCutcheon, J. R. Relating osmotic performance of thin film composite hollow fiber membranes to support layer surface pore size. *J. Membr. Sci.* **2017**, *540*, 344−353.
(20) Koros, W. J.; Woods, D. G. Elevated temperature application of polymer hollow-fiber membranes. *J. Membr. Sci.* **2001**, *181* (2), 157−166.
(21) Ali, Z.; Pacheco, F.; Litwiller, E.; Wang, Y.; Han, Y.; Pinnau, I. Ultra-selective defect-free interfacially polymerized molecular sieve thin-film composite membranes for H_2 purification. *J. Mater. Chem. A* **2018**, *6* (1), 30−35.
(22) Iyer, G. M.; Liu, L.; Zhang, C. Hydrocarbon separations by glassy polymer membranes. *J. Polym. Sci.* **2020**, *58* (18), 2482−2517.
(23) Petersen, J.; Peinemann, K.-V. Novel polyamide composite membranes for gas separation prepared by interfacial polycondensation. *J. Appl. Polym. Sci.* **1997**, *63* (12), 1557−1563.
(24) Sanders, D. F.; Smith, Z. P.; Guo, R.; Robeson, L. M.; McGrath, J. E.; Paul, D. R.; Freeman, B. D. Energy-efficient polymeric gas separation membranes for a sustainable future: A review. *Polymer* **2013**, *54* (18), 4729−4761.
(25) Ekiner, O. M.; Vassilatos, G. Polymeric membranes. U.S. Patent No. US5085774, 1992.
(26) Geise, G. M.; Park, H. B.; Sagle, A. C.; Freeman, B. D.; McGrath, J. E. Water permeability and water/salt selectivity tradeoff in polymers for desalination. *J. Membr. Sci.* **2011**, *369* (1), 130−138.
(27) White, H. D.; Li, C.; Lively, R. P. Tailoring the Structure of Carbon Molecular Sieves Derived from an Aromatic Polyamide. *Ind. Eng. Chem. Res.* **2022**, *61* (15), 5314−5323.
(28) Gu, J.-E.; Lee, S.; Stafford, C. M.; Lee, J. S.; Choi, W.; Kim, B.-Y.; Baek, K.-Y.; Chan, E. P.; Chung, J. Y.; Bang, J.; Lee, J.-H. Molecular Layer-by-Layer Assembled Thin-Film Composite Membranes for Water Desalination. *Adv. Mater.* **2013**, *25* (34), 4778−4782.
(29) Kwolek, S. L.; Morgan, P. W. Preparation of polyamides, polyurethanes, polysulfonamides, and polyesters by low temperature solution polycondensation. *J. Polym. Sci., Part A: Gen. Pap.* **1964**, *2* (6), 2693−2703.
(30) Shawky, H. A. Performance of aromatic polyamide RO membranes synthesized by interfacial polycondensation process in a water-tetrahydrofuran system. *J. Membr. Sci.* **2009**, *339* (1), 209−214.
(31) Ekiner, O. M.; Vassilatos, G. Polyaramide hollow fibers for hydrogen/methane separation—spinning and properties. *J. Membr. Sci.* **1990**, *53* (3), 259−273.
(32) Robeson, L. M. The upper bound revisited. *J. Membr. Sci.* **2008**, *320* (1), 390−400.
(33) Hatori, H.; Takagi, H.; Yamada, Y. Gas separation properties of molecular sieving carbon membranes with nanopore channels. *Carbon* **2004**, *42* (5), 1169−1173.
(34) Hosseini, S. S.; Chung, T. S. Carbon membranes from blends of PBI and polyimides for N_2/CH_4 and CO_2/CH_4 separation and hydrogen purification. *J. Membr. Sci.* **2009**, *328* (1), 174−185.
(35) Lei, L.; Pan, F.; Lindbråthen, A.; Zhang, X.; Hillestad, M.; Nie, Y.; Bai, L.; He, X.; Guiver, M. D. Carbon hollow fiber membranes for a molecular sieve with precise-cutoff ultramicropores for superior hydrogen separation. *Nat. Commun.* **2021**, *12* (1), 268.
(36) Campo, M. C.; Magalhães, F. D.; Mendes, A. Carbon molecular sieve membranes from cellophane paper. *J. Membr. Sci.* **2010**, *350* (1-2), 180−188.
(37) Sanyal, O.; Hays, S. S.; León, N. E.; Guta, Y. A.; Itta, A. K.; Lively, R. P.; Koros, W. J. A Self-Consistent Model for Sorption and Transport in Polyimide-Derived Carbon Molecular Sieve Gas Separation Membranes. *Angew. Chem., Int. Ed.* **2020**, *59* (46), 20343−20347.
(38) Bénard, P.; Chahine, R. Determination of the Adsorption Isotherms of Hydrogen on Activated Carbons above the Critical Temperature of the Adsorbate over Wide Temperature and Pressure Ranges. *Langmuir* **2001**, *17* (6), 1950−1955.
(39) Weinkauf, D. H.; Kim, H. D.; Paul, D. R. Gas transport properties of liquid crystalline poly(*p*-phenyleneterephthalamide). *Macromolecules* **1992**, *25* (2), 788−796.
(40) Steel, K. M.; Koros, W. J. An investigation of the effects of pyrolysis parameters on gas separation properties of carbon materials. *Carbon* **2005**, *43* (9), 1843−1856.
(41) Araújo, T.; Andrade, M.; Bernardo, G.; Mendes, A. Stable cellulose-based carbon molecular sieve membranes with very high selectivities. *J. Membr. Sci.* **2022**, *641*, 119852.
(42) Thommes, M.; Kaneko, K.; Neimark, A. V.; Olivier, J. P.; Rodriguez-Reinoso, F.; Rouquerol, J.; Sing, K. S. W. Physisorption of gases, with special reference to the evaluation of surface area and pore size distribution (IUPAC Technical Report). *Pure Appl. Chem.* **2015**, *87* (9−10), 1051−1069.

https://doi.org/10.1021/acsmaterialslett.2c01029
ACS Materials Lett. 2023, 5, 243−248